Porosity reduction possibilities in commercial Aluminium A380 and Magnesium AM60 alloy components using the RheoMetal™ process

Olof Granath, Magnus Wessén and Haiping Cao
Jönköping University, Div. Materials and Manufacturing SE-551 11 Jönköping, Sweden

ABSTRACT

A commercial component was produced from both aluminium A380 (EN AC 46000) and magnesium AM60 alloys by high pressure die casting (HPDC) and rheocasting using the RheoMetal process. This process, which is based on the Rapid Slurry Forming (RSF) technology, is capable of producing large amounts of metal slurries in short times. The aim of this paper is to investigate the possibility to reduce porosity, and the related effects on the tensile properties obtained in RSF rheocast components. Significantly reduced pore content was obtained in the RSF rheocast A380 and AM60 alloy components, as compared to the HPDC components. This was confirmed by X-ray analysis, microstructure analysis and on polished component sections. The turbulent filling behaviour in HPDC produces severe amounts of entrained gas type porosity. It was also found that gas pores often were connected to shrinkage type pores.

RIASSUNTO

È stato prodotto un componente commerciale in lega sia di Alluminio A380 (EN AC 46000) anche di Magnesio AM60 mediante le tecniche di colata ad alta pressione e di reocolata, usando il processo RheoMetal. Questo processo, basato sulla tecnologia Rapid Slurry Forming (RSF), consente di produrre notevoli quantità di "slurry" in tempi brevi. Il lavoro ha lo scopo di investigare la possibilità di ridurre la porosità e quindi gli effetti che da essa dipendono sulle proprietà tensili in componenti ottenuti via RSF. Rispetto ai componenti prodotti per colata ad alta pressione, quelli ottenuti per reocolata delle due leghe sottoposte a RSF presentano una notevole riduzione di porosità. Questo risultato è stato confermato dalle analisi microstrutturali e ai raggi X eseguite su sezioni del componente. Il riempimento turbolento dello stampo nella colata ad alta pressione produce notevoli quantità di porosità per intrappolamento di gas. È stato infine provato che i pori da gas sono spesso connessi a quelli da ritiro.

KEYWORDS

Semi-solid, rheocasting, RheoMetal, RSF, porosity reduction, tensile property.

INTRODUCTION

Semi-solid casting is characterised by a process that uses a partially solidified metal alloy having a globular microstructure, also known as slurry, to produce cast components. The main routes of semi-solid casting are thixocasting and rheocasting. Thixocasting is the forming of components from reheated billets in the semi-solid state. Rheocasting is the production of semi-solid slurry from a melt followed by component casting. The semi-solid route considered in this paper is rheocasting. Some of the known rheocasting processes to date are; NRC [1], SLC [2], DSF [3], CRP [4], SEED [5], SSR [6], Thixomolding [7, 8] and Rheo-Diecasting [9].

The recently developed RheoMetal™ process, based on the Rapid Slurry Forming (RSF) technology, differs from other rheocasting processes in that heat extraction by external cooling is not necessary. It involves an enthalpy exchange between two alloy systems where one alloy is the superheated melt and the other is the cold solid Enthalpy Exchange Material (EEM) alloy piece, which is immersed and stirred in the melt. During stirring, melting and dissolution of the EEM occurs quickly, thereby forming metal slurry. As a consequence, a new alloy system will form with a certain enthalpy and solid fraction. Detailed descriptions of the RSF technology were presented at the 3rd HTDC conference in 2006 [10-11].

The major advantage of semi-solid casting compared to high pressure die casting (HPDC) is a reduced porosity level, which gives several advantages; such as heat treatability, pressure tightness, weldability and smooth surfaces even in machined areas of a casting. It was found that porosity levels in HPDC (A380 alloy) and semi-solid castings (A356 alloy) were as different as 2.36% and 0.17% respectively [12]. Rheocast A357 alloy components were found to have high material density compared to those cast from liquid melts [13]. Large amounts of porosity were discovered in die cast as well as in thixomolded magnesium AM60 and AZ91 components [7]. Thixomolded components have also been shown to have larger porosity amounts for an increased component wall thickness [8]. Some other advantages associated with semi-solid casting, such as near net shape and increased die life, have been described in detail elsewhere [14].

The commercial aluminium A380 HPDC alloy is normally difficult to cast by semi-solid processing as its solidification interval is smaller than the more favoured A356 type alloys. Most investigations are therefore focused on microstructure evaluation rather than the castability and tensile properties of A380 alloys [4, 6]. Considering the castability difference between semi-solid magnesium and aluminium alloys, it has been shown that semi-solid magnesium alloys have a larger freezing tendency that may cause difficulties during mould filling [15].

Observations in the present work arise from RSF rheocasting trials and HPDC reference trials where a commercial component was produced using aluminium A380 and magnesium AM60 alloys. The aim of this study was to investigate the possibility to reduce porosity, and the related effects on the tensile properties obtained in RSF rheocast components.

EXPERIMENTAL PROCEDURE

In this study two different alloys have been used to produce commercial components in open atmosphere trials by either HPDC or rheocasting according to the principles of the RSF technology. The alloy selected for all aluminium trials was A380 (EN AC 46000). An AM60 alloy was used in all magnesium trials. The chemical compositions of these alloys are shown in table 1.

Table 1. The chemical compositions of the A380 and AM60 alloys used

	Al	Si	Fe	Cu	Mn	Mg	Ti	Sr	Zn
A380 HPDC	Bal.	8.10	0.87	2.37	0.20	0.35	0.030	0.0003	1.13
A380 RSF	Bal.	8.90	0.89	2.28	0.33	0.22	0.035	0.0005	0.64
	Mg	**Al**	**Mn**	**Zn**	**Si**	**Fe**	**Cu**	**Ni**	**Pb**
AM60 HPDC	Bal.	5.61	0.30	0.045	0.044	0.001	0.005	0.008	0.013
AM60 RSF	Bal.	5.90	0.29	0.038	0.049	0.002	0.005	0.006	0.010

The RSF aluminium rheocasting trial, the HPDC aluminium trial and the HPDC magnesium trial were performed using a cold chamber high pressure die casting machine having a 500-tonne locking force. A 650-tonne cold chamber high pressure die casting machine was used in the RSF rheocasting magnesium trial. The various shot weights and machine parameters used are shown in table 2. The aluminium and magnesium HPDC reference components were cast with the original gating system of the die. Melt dosing was done with the automatic equipment provided by the machine. Prior to the RSF A380 rheocasting trial the gating system of the die was modified according to semi-solid casting requirements. The gating system had to be modified once more for the AM60 RSF trial to account for the lower heat content of magnesium alloys. Melt dosing in the RSF trials was done manually in a 152mm (outer diameter) graphite crucible having a 12mm wall thickness. That crucible could contain a maximum of 3.2kg or 2.1kg of molten aluminium or magnesium respectively. After correct melt dosing a 38mm diameter EEM, with its height dimensioned for the EEM to be approximately 5 wt% of the melt weight, was immersed into the melt and stirred at a rotation rate of 1200 rpm for no more than 15 seconds to produce slurry. After its formation the slurry was manually poured from the crucible into the shot sleeve of the machine for injection into the die cavity.

The commercial component with its regions of interest for this study is depicted in fig. 1. Samples for microscopy investigation were

taken from the main plate and the tower. Normal metallographic procedures for aluminium and magnesium alloys were followed during sample preparation and polishing. All magnesium samples needed to be etched to reveal the morphology of the primary grains. Microstructures were studied using a Leica DMRX optical microscope. At least 500 globules (i.e. the primary phase) were measured when estimating globule sizes in each typical component region. A measurement technique was used that required two transversal lengths of perpendicular direction to be drawn in order to acquire the size of each globule. X-ray analysis was used to investigate porosity contents after each trial. Different sections of the T-bar of a few selected components from each batch were polished to reveal any porosity. The front view of the component is depicted in fig. 2 where the two area markings show from where tensile test specimens were taken. The dimensions of these specimens are shown in fig. 3. Five components, having equal biscuit thickness, were selected from each A380 HPDC and RSF trial for evaluation. One component from the AM60 trial was evaluated for each production method. Four tensile test specimens were taken from each component selected. The crosshead velocity of the tensile test machine was 0.5mm per minute when applying an increasing load until the specimen fractured. The gauge length of the clip-on type extensometer used was 20mm.

Table 2. Shot weights and various machine parameters used in this work

	Unit	A380 HPDC	A380 RSF	AM60 HPDC	AM60 RSF
Shot weight	[kg]	2.3	2.6	1.5	1.9
Piston diameter	[mm]	80	80	80	80
Piston velocity, 1st phase	[m/s]	0.5	0.3-0.5	0.5	0.5-0.7
Piston velocity, 2nd phase	[m/s]	3.5	N/A	3.5	N/A
Shot sleeve length	[mm]	500	500	500	460
Intensification pressure	[bar]	220	150	200	130
Furnace temperature	[°C]	720	640	710	655

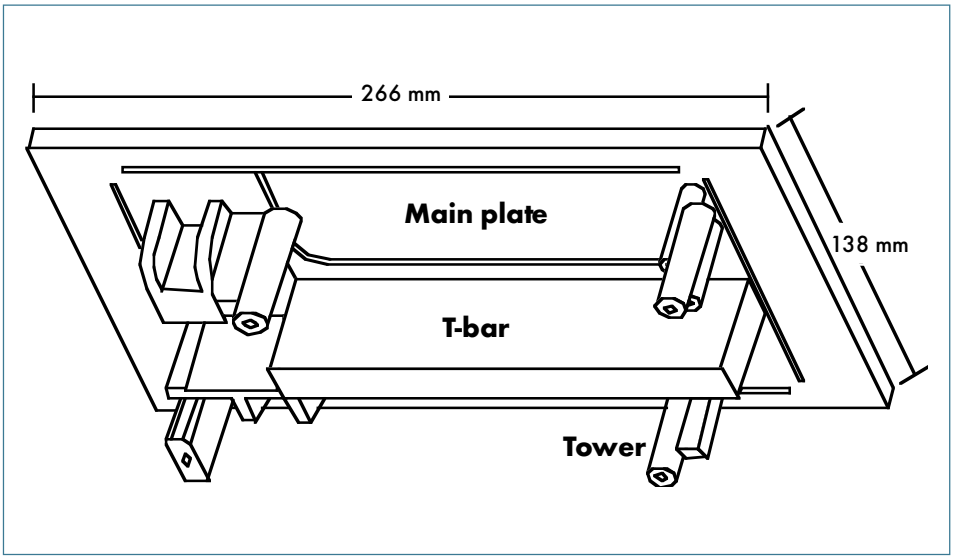

Fig. 1: Some dimensions of the commercial component. Main plate thickness is 10 mm.

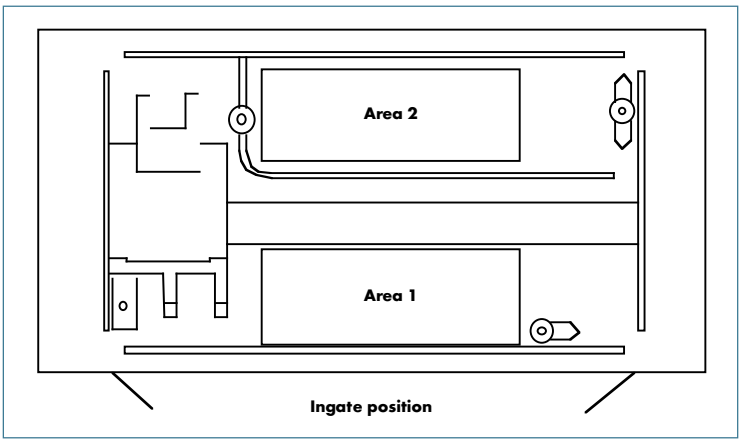

Fig. 2: Front view showing the areas in the main plate from where tensile test specimens were taken.

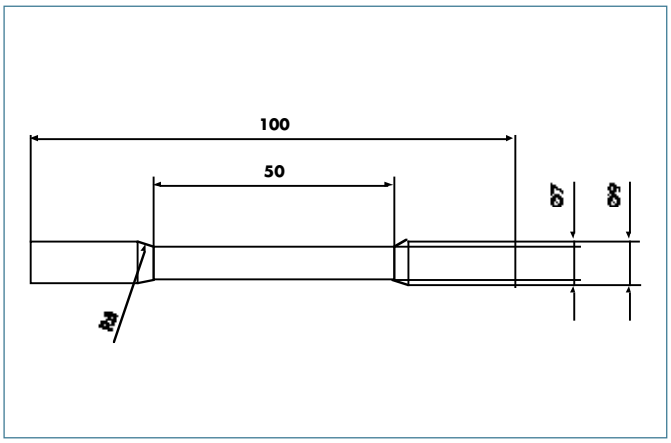

Fig. 3: The dimensions of the tensile test specimen.

RESULTS AND DISCUSSION

ALUMINIUM A380 TRIALS

This first part of the paper deals with the results obtained from the aluminium alloy trials. The liquidus temperature of the A380 alloy was estimated from cooling curve analysis to be approximately 591°C. In the A380 RSF rheocasting trials the temperature after slurry formation, before pouring the slurry into the shot sleeve, was around 585°C. This casting temperature is typically about 100°C lower than in HPDC. It should be emphasized that the use of such low casting temperatures has many positive effects on the casting process. In particular this relates to a prolonged die life and reduced cycle times; especially for more bulky components. Additionally, it can be assumed that the temperature variations in the tool are reduced, meaning that less thermal stresses are likely to build up; both in the tool itself, but also in the casting.

Microstructures from HPDC and RSF aluminium alloy components have fundamentally different primary morphologies; dendritic and globular respectively. Two typical micro structures taken from the main plate and tower regions of the HPDC components are shown in fig. 4. These microstructures are very similar. A fine dendritic structure is formed in both the tower and the main plate region, indicating a quick solidification during processing. Microstructures typical for RSF rheocast components are shown in fig. 5. The globule size of the main plate and tower regions were evaluated to be; 64±5 µm and 60±5 µm respectively. This small difference in globule size makes the microstructures in the component to be rather uniform. From these RSF micrographs it is also clear that the eutectic structure of the main plate and tower regions are quite similar.

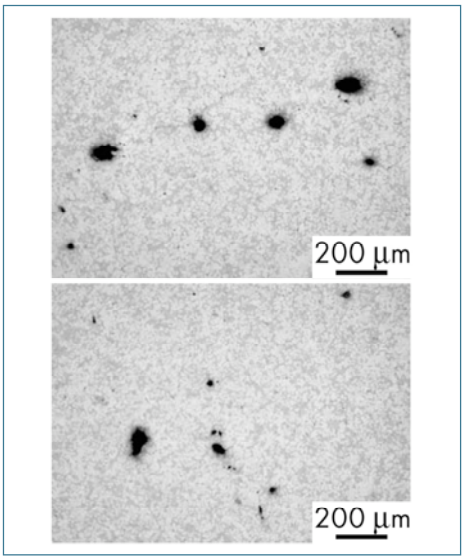

Fig. 4: A380 HPDC microstructures taken from the main plate (top) and the tower (bottom).

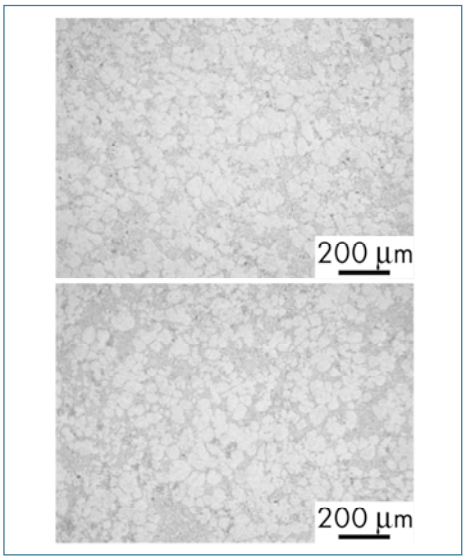

Fig. 5: A380 RSF rheocast microstructures taken from the main plate (top) and the tower (bottom).

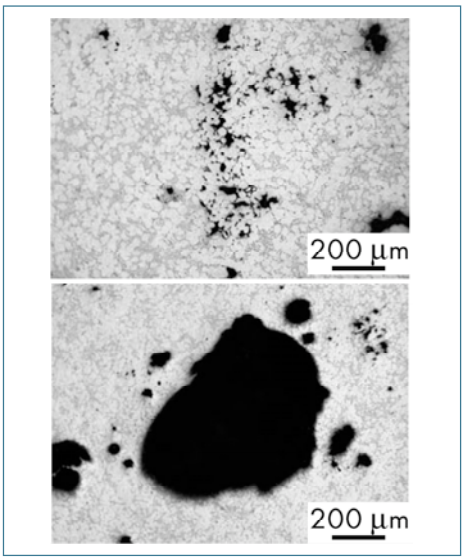

Fig. 6: Typical defects shown in the microstructure of the main plate (top) and the tower (bottom) of A380 HPDC samples. Note the difference in magnification.

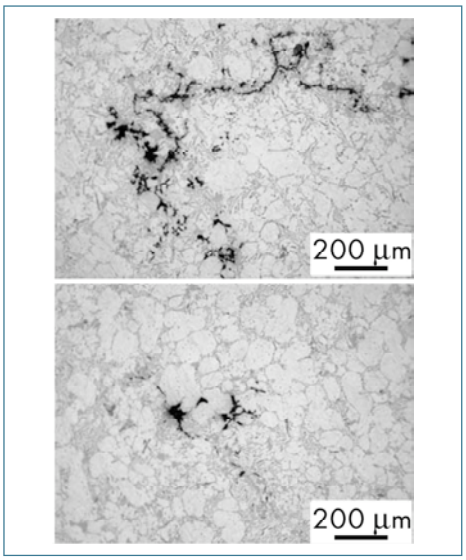

Fig. 7: Defects found in the microstructure of the main plate (top) and the tower (bottom) of A380 RSF rheocast samples.

An obvious difference in the degree of porosity between HPDC and RSF materials is observed when studying the micrographs in fig. 4 and 5. When investigating the main plate and tower region microstructures two different types of porosity were found in HPDC components; shrinkage porosity (irregularly shaped) and gas porosity (spherically shaped), see fig. 6. The severe amounts of gas porosity formed depend on the die filling turbulence associated with the HPDC process. Gas and shrinkage pores were often connected, which suggests that gas porosity may act as a nucleation site for shrinkage porosity. As a large number of small gas bubbles are present in the liquid after the turbulent die filling procedure, these may agglomerate to form larger bubbles under the high pressure applied during solidification. During the shrinkage of the melt, the related porosities formed are likely to precipitate onto the existing gas pores. Under such conditions gas pores may also nucleate at defects such as oxide films. Hydrogen dissolved in the melt is another possible source for the porosity. In the RSF rheocast sample microstructures only shrinkage type

porosities were found as shown in fig. 7. The shrinkage porosity discovered in the main plate was the largest porosity found. Smaller pores, as found in the tower region, are far more representative for RSF components. The lower amount of porosity found in RSF components is likely to be an effect of not only the laminar die filling behaviour but also of the globular morphology of the primary phase, which provides improved feeding during solidification.

Evidence of improved component quality (reduced porosity) is given by the X-ray images of HPDC and RSF components shown in figs. 8 and 9. The HPDC components show a significantly larger amount of porosity than do the RSF components. Furthermore, the porosity distribution seems to be non-uniform in the HPDC components, again suggesting turbulence related origins.

One of the most difficult component regions to cast with high integrity using HPDC was the T-bar. Because of the T-bar design, the formation of a hot spot in the junction with the main plate causes severe porosity. Another design feature contributing to porosity in that junction is that the main plate is thinner than the T-bar, which results in insufficient feeding during solidification. The significant porosity reduction in the T-bar region using RSF rheocasting is clear from the sections shown in fig. 10. The HPDC components produced show a non-uniform porosity distribution and large irregular pores in this region. Evidently, a less turbulent die filling behaviour and a globular structured material is successful in strongly reducing porosity in regions that are difficult to cast, even if porosity is not fully eliminated. This is due to an incorrect component design. Porosity is also decreased by the strongly reduced solidification shrinkage obtained as the slurry contains a large amount of pre-solidified primary phase. The minor amount of porosity seen in the junction hot spot of the RSF component can most likely be further reduced with improved feeding by; (1) applying a higher intensification pressure and (2) making further modifications to the ingate and gating system of the die.

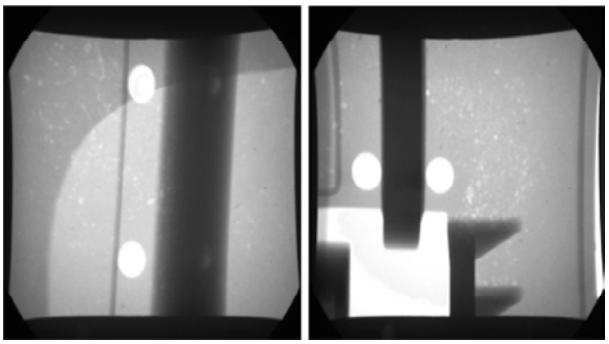

Fig. 8: X-ray images of HPDC A380 alloy components.

Fig. 9: X-ray images of RSF rheocast A380 alloy components.

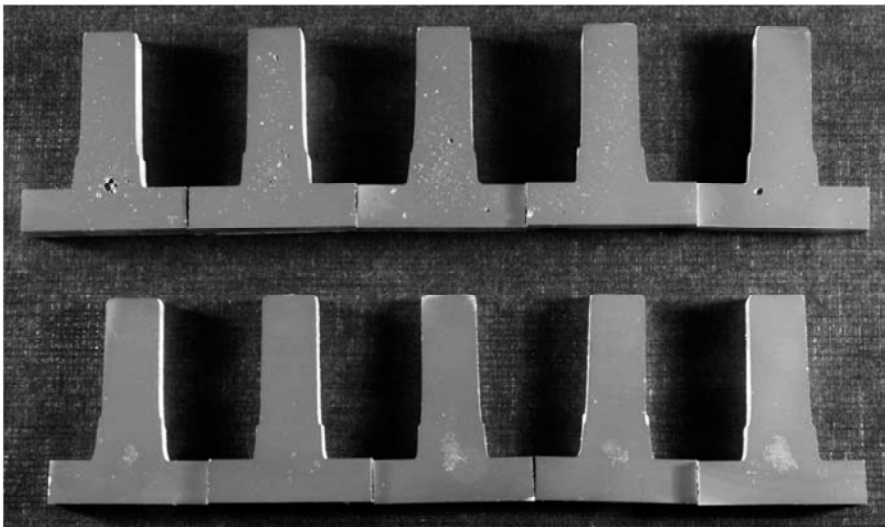

Fig. 10: Different examples of the T-bar in HPDC (top) and RSF (bottom) A380 alloy components.

The significantly reduced porosity in the RSF components is illustrated by the surfaces of the machined tensile test specimens, taken from the main plate of the components; see figs. 11 and 12. Not one single pore was found on any of the RSF specimens shown in fig. 12. From this it is easy to understand that the RSF material also can be used in a fully heat treated state (T6), without having the problems related to blistering, thereby obtaining a further significant improvement in mechanical properties.

The average tensile properties, including standard deviations, of the A380 alloy components produced by the two different processes are summarised in table 3. A small influence of the different chemical compositions and processing conditions, leading to different formation of intermetallic phases in the microstructure, is naturally expected for the A380 alloy. It is interesting to note that the Young's modulus is higher for the RSF materials, and that its standard deviation is significantly smaller than that of the HPDC specimens. It is reasonable to assume that this effect can be attributed to the lower pore content in the RSF materials. The 0.2% proof stress for the HPDC and RSF materials do not however seem to be influenced by porosity. The elongation of the RSF material is only slightly higher than that of the HPDC material for an identical standard deviation. It is assumed that porosity may have an influence on these results as the porosity amounts, pore sizes and connected types of porosity are different for the two materials. The influence of intermetallic phases may also have an effect on properties as found by other researchers [16]. The best elongation obtained for HPDC as well as for RSF materials was approximately 2% and is presented in the tensile test curves in fig. 13. Maximum elongation for an A380 alloy, obtained by a gradient solidification technique, is in the range of 5 to 8% for a sample with secondary dendrite arm spacing (SDAS) representative of a HPDC sample [16]. As the experiments described in the present paper were made in open atmosphere, oxides will exist in all castings produced. Since many similar properties

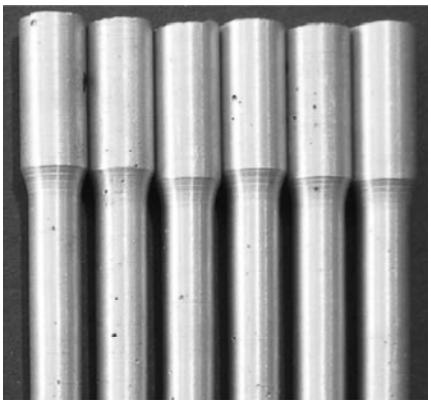

Fig. 11: A380 HPDC tensile test specimens.

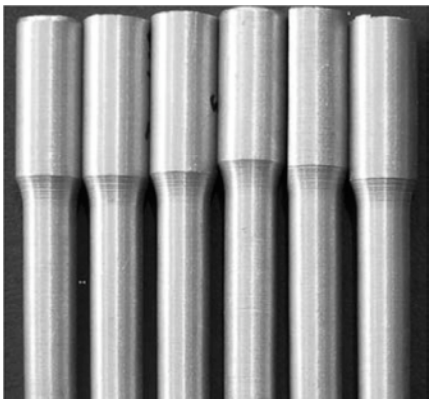

Fig. 12: A380 RSF tensile test specimens.

Table 3. Average tensile properties and standard deviations obtained from A380 alloy components

	Young's modulus [GPa]	0.2% proof stress [MPa]	Fracture stress [MPa]	Elongation [%]
A380 HPDC	67.4±3.8	122.7±5.7	176.0±23.1	1.2±0.4
A380 RSF	72.5±1.0	118.3±8.3	183.7±19.1	1.4±0.4

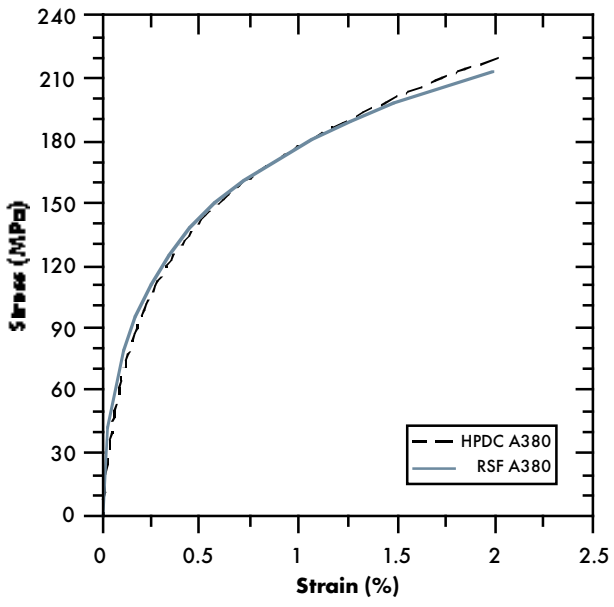

Fig. 13: Tensile test curves showing the maximum elongations obtained in A380 components.

were found for the two production processes tested, the effect of oxides on properties should be similar in the HPDC and RSF materials. As a consequence, no major effect on tensile properties of the primary morphology could be verified.

MAGNESIUM AM60 TRIALS

This second part of the paper considers magnesium AM60 alloy components produced by HPDC and RSF rheocasting. First of all it should be emphasized that also the Mg-slurry was produced without haing any protective atmosphere. As a consequence, the melt oxidized severely during melt handling, especially during the slurry forming step. Further, it needs to be repeated that only one component from each small batch of HPDC and RSF components was selected, due to production stability difficulties caused by the oxidization. Only a limited number of conclusions can therefore be drawn.

The liquidus temperature of the AM60 alloy of 619°C was estimated from cooling curve analysis. In the AM60 RSF trial the slurry temperature obtained before pouring the slurry into the shot sleeve was approximately 615°C, which is significantly lower than the casting temperatures used in HPDC.

Representative microstructures from the main plate and tower regions of the HPDC and RSF rheocast components are shown in figs. 14 and 15 respectively. The dendritic morphology of the HPDC component display some larger grains most likely pre-solidified in the shot sleeve of the high pressure die casting machine. This is an expected problem in HPDC cast magnesium alloys because of their sensitivity to heat losses. Based on the size of these pre-solidified grains it is likely that some effect, beyond that of the ordinary dendritic morphology, on feeding during solidification may exist. The two HPDC regions investigated display similar microstructures. RSF rheocast microstructures show a primary globular morphology, free from any large grains solidified in the shot sleeve. Similar to the aluminium trials the globule size difference between the main plate (57±6 μm) and the tower (54±6 μm) is small, showing the globule size in the component to be rather uniform.

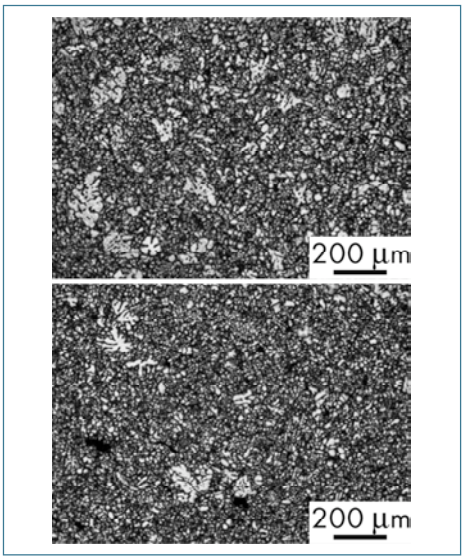

Fig. 14: AM60 HPDC microstructures taken from the main plate (top) and the tower (bottom).

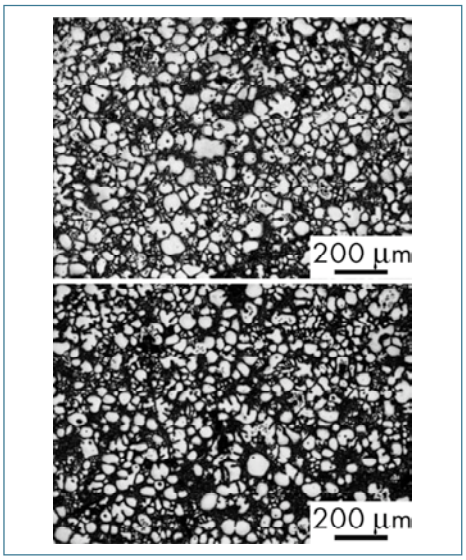

Fig. 15: AM60 RSF rheocast microstructures taken from the main plate (top) and the tower (bottom).

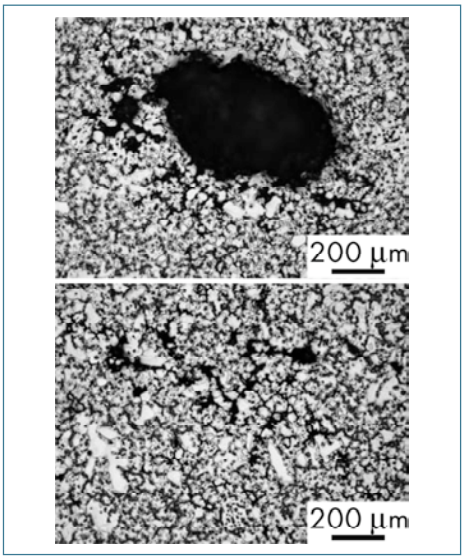

Fig. 16: Typical defects found in the microstructure of the main plate (top) and the tower (bottom) of AM60 HPDC samples.

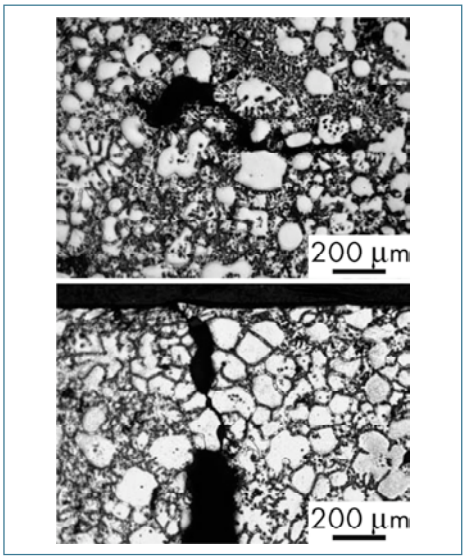

Fig. 17: Defects found in the microstructure of AM60 RSF rheocast samples; main plate (top) and tower (bottom).

Two types of porosity, similar to that caused by gas or shrinkage, were well represented in the HPDC microstructures as shown in fig. 16. The gas type pores found in the main plate region were occasionally very large in size. Some pores have been found close to the larger pre-solidified grains. Gas type pores were commonly connected to shrinkage type porosity. Generally, the gas porosities found in the HPDC samples can be related to turbulent die filling. In the RSF rheocast component shrinkage pores were the only porosity found, as shown in fig. 17. A crack was found close to the casting surface in the tower (fig.

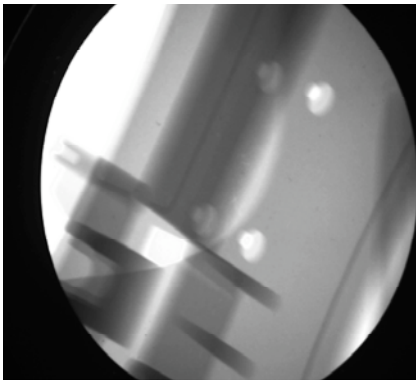

Fig. 18: X-ray image of a HPDC AM60 component.

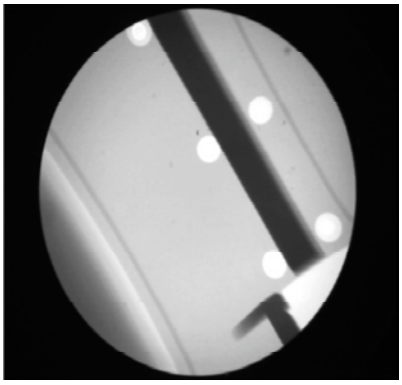

Fig. 19: X-ray image of a RSF AM60 component.

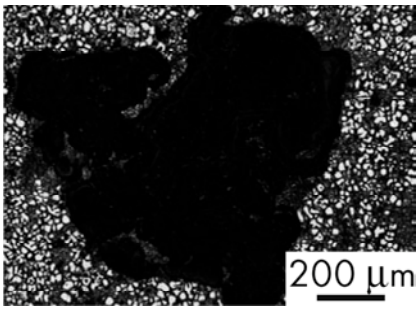

Fig. 20: A large iron flake found in an AM60 RSF rheocast component.

17, bottom). It is reasonable to assume that this is caused by either; (1) a weld line formed from two filling fronts which widened during solidification or (2) a hot tear.

X-ray analysis revealed that the HPDC component had porosity mostly in and underneath the T-bar as shown in fig. 18. Evidence of low porosity in the RSF component is given by the X-ray image provided in fig. 19. The small black impurities observed in the RSF X-ray image are iron flakes from the iron crucible. Naturally, these flakes should not be considered to be related to the slurry production. Presented in fig. 20 is a large iron flake from the rheocast component. The effect caused by these flakes on porosity formation should be large as they reduce feeding paths during solidification due to their extremely large size. However, pores were not frequently found around these flakes.

The sections taken from the T-bar region of the HPDC and the RSF component are shown in fig. 21. It is evident that RSF rheocasting reduces porosity compared to HPDC. Large and spherically shaped pores were found in the HPDC sections. These pores are related to severe air entrapment caused by a turbulent die filling. Some iron flakes are visible in the RSF component sections that can easily be mistaken for porosity. The highly modified gating system used in the RSF AM60 trials has contributed to reduced porosity in the junction hot spot below the T-bar. This finding reveals gating system design possibilities to improve feeding in RSF rheocasting.

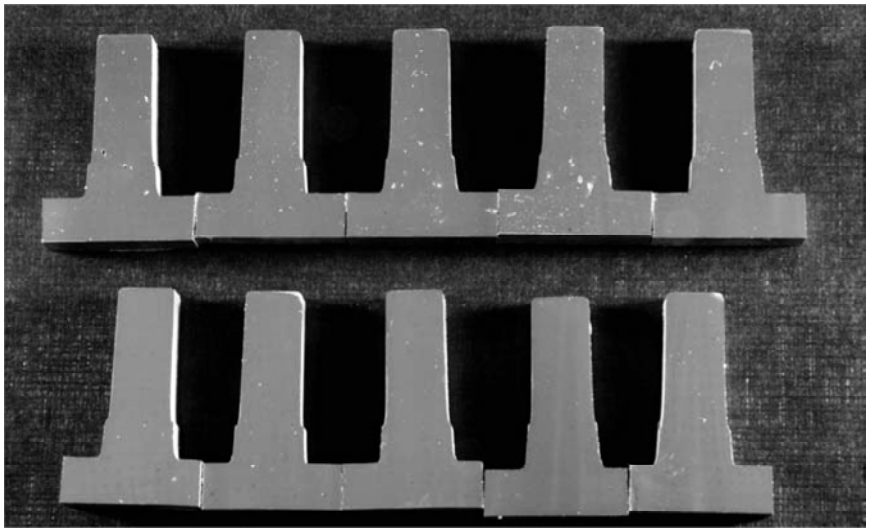

Fig. 21: Different examples of the T-bar in HPDC (top) and RSF (bottom) AM60 alloy components.

Table 4. Average tensile properties and standard deviations obtained from AM60 alloy components

	Young's modulus [GPa]	0.2 % proof stress [MPa]	Fracture stress [MPa]	Elongation [%]
AM60 HPDC	40.4±2.1	95.9±5.0	149.0±27.1	2.7±1.2
AM60 RSF	40.0±1.3	92.2±1.2	143.3±13.0	2.1±0.7

The average tensile properties of HPDC and RSF AM60 alloys are compared in table 4. Based on these results, the main plate regions of the HPDC and the RSF component clearly have similar properties. In fig. 22 the tensile test curves having the highest elongation for each material are shown. Obviously the deformation behaviour, i.e. the 0.2% proof stress and the strain hardening, for the two materials are very similar. However, the elongation at fracture is slightly lower for the RSF material. Two possible causes for the unexpected reduced elongation in RSF materials are suggested, (1) the presence of iron flakes and (2) oxides. Iron flakes will be detrimental to tensile properties as they will induce stresses because of their large size and complex shape. The sensitivity to oxidization of magnesium alloys combined with an open atmosphere trial procedure will entrap oxides in the component. Elongations higher than 10% have been obtained for an AM60 type alloy using a gradient solidification technique [17]. The decreased porosity possible by RSF rheocasting presents a great potential for structural magnesium applications. However, improvements of the processing conditions are needed in order to obtain better tensile properties.

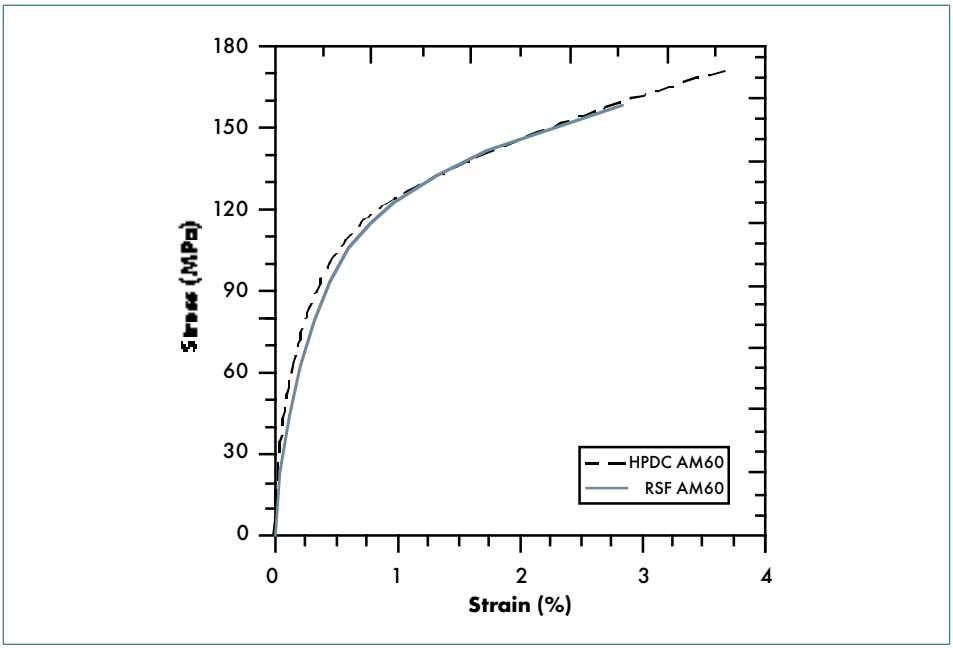

Fig. 22: AM60 tensile test curves showing the maximum elongations obtained.

CONCLUSIONS

The following conclusions can be drawn:

- Aluminium A380 (EN AC 46000) and magnesium AM60 alloys can be rheocast using the RSF technology and the RheoMetal™ process. Magnesium alloys present more production stability difficulties than aluminium alloys.
- Rheocasting according to the principles of the RSF technology significantly reduced porosity in the A380 and AM60 alloy components produced.
- The different filling behaviour of RSF rheocasting and HPDC causes different types of porosity to form in the casting. Apart from porosity having shrinkage type characteristics, turbulence causes entrapped gas porosity in HPDC castings. Gas porosity was commonly connected with shrinkage type porosity in HPDC castings.
- Significantly decreased casting temperatures can be used to produce cast components with the RSF technology.
- Globule sizes in RSF rheocast components were fine and with only small differences between the regions investigated.
- The processing conditions of RSF magnesium rheocasting needs to be improved to provide an oxide free environment.

ACKNOWLEDGEMENTS

The authors wish to express their sincere gratitude to Finnveden Metal Structures AB and Stena Aluminium AB for support and providing materials for the experiments, to the Swedish Agency for Innovation Systems (VINNOVA) and the Programme for Vehicle Research (PFF) for financially sponsoring the project. Furthermore, Mr. Leif Andersson of Jönköping University is greatly acknowledged for participation in the trials performed.

REFERENCES

[1] Adachi M. and Sato S. Characteristics of the New Rheocasting process. Proc. 20th Int. Die Casting Cong., NADCA Cong., Cleveland, OH, USA, November 1-4, (1999), 47-52.

[2] Jorstad J., Thieman M., Kamm R., Loughman M. and Woehlke T. Sub Liquidus Casting (SLC): Process, Concept and Product. Trans. American Foundry Society and the One Hundred Seventh Annual Casting Cong., Milwaukee, WI, USA, April 26-29, (2003), 399-405.

[3] Rice C.S. and Mendez P.F. Slurry-based semi-solid die casting. Advanced Materials and Processes 159 no. 10, (2001), 49-52.

[4] Pan Q.Y., Apelian D. and Hogan P. The Continuous Rheoconversion Process (DRPTM): optimization & industrial applications. Proc. 3rd Int. Conf. on High Tech Die Casting, AIM, Vicenza, Italy, September 21-22, (2006).

[5] Doutre D., Hay G., Wales P. and Gabathuler J.-P. SEED: A new process for semi solid forming. Light Metals 2003 (Métaux Légers) Proc. 42nd Annual Conf. of Metallurgists of CIM: Int. Symposium on Light Metals, Vancouver, Canada, August 24-27, (2003), 293-306.

[6] Yurko J.A., Martinez R.A. and Flemings M.C. Commercial development of the semi-solid rheocasting (SSRTM) process. Metallurgical Science and Technology 21 no.1, (2003), 10-15.

[7] Thoma P.E., Hayes C. and Baik A. The influence of microstructure on the fracture and tensile properties of die cast and thixomolded magnesium alloys. Materials Research Society Symposium 539, (1999), 35-40.

[8] Lohmüller A., Scharrer M., Jenning R., Hilbinger M., Hartmann M. and Singer R.F. Injection molding of magnesium alloys. Proc. 6th Int. Conf. Magnesium Alloys and their Applications, Wolfsburg, November 18-20, (2003), 738-743.

[9] Fan Z., Ji S., and Liu G. Development of the Rheo-Diecasting process for Mg-alloys. Materials Science Forum 488-489, (2005), 405-412.

[10] Granath O., Wessén M. and Cao H. Influence of holding time on particle size of an A356 alloy using the new Rapid Slurry Forming process. Proc. 3rd Int. Conf. on High Tech Die Casting, AIM, Vicenza, Italy, September 21-22, (2006).

[11] Wessén M. and Cao H. The RSF technology – a possible breakthrough for semi-solid casting processes. Proc. 3rd Int. Conf. on High Tech Die Casting, AIM, Vicenza, Italy, September 21-22, (2006).

[12] Hairy P., Laguerre C., Longa Y., Cuche G., Sportelli J., Garat M., Brimont M., Guillet S. and Franchet B. Thixocasting: comparison of foundry processes on a test casting. Fonderie Foundour d'Aujourd'hui 210, (2001), 13-20.

[13] Basner T. Rheocasting of semi-solid A357 aluminum. SAE World Cong., Detroit, MI, USA, March 6-9, (2000), paper no. 2000-01-0059.

[14] Flemings M.C. Behavior of metal alloys in the semisolid state. Metallurgical and Materials Transactions A 22A, (1991), 957-981.

[15] Uggowitzer P.J., Gullo G.-C. and Wahlen A. Metallkundliche Aspekte bei der semi-solid Formgebung von Leichtmetallen. Vom Werstoff zum Bauteil (Ed. Kaufmann H. and Uggowitzer P.J.), LKR-Verlag Ranshofen, May (2000), 95-107.

[16] Seifeddine S., Sjögren T. and Svensson I.L. The influence of Al5FeSi on the tensile properties of a HPDC cast aluminium alloy – potential and outcome in a casting. Proc. 2nd Int. Conf. on High Tech Die Casting, AIM, Brescia, Italy, April 21-22, (2004).

[17] Cao H. and Wessén M. Effect of microstructure on mechanical properties of as-cast Mg-Al alloys. Metallurgical and Materials Transactions A 35A, (2004), 309-319.